OCEANIC BOUNDARY CURRENTS

**Shiro IMAWAKI [1], Walter ZENK [2], Susan WIJFFELS [3],
Dean ROEMMICH [4] and Masaki KAWABE [5]**

[1] *Research Institute for Applied Mechanics, Kyushu University, Kasuga, Japan*
[2] *Institut fuer Meereskunde an der Universitaet Kiel, Kiel, Germany*
[3] *Commonwealth Science and Industry Research Organization, Hobart, Australia*
[4] *Scripps Institution of Oceanography, La Jolla, USA*
[5] *Ocean Research Institute, University of Tokyo, Tokyo, Japan*

ABSTRACT - *Measurements of oceanic boundary current for integral quantities such as heat and freshwater fluxes are very important for studying its long-term impact on the global climate. There are a variety of boundary currents, including surface, intermediate and deep boundary currents on both western and eastern sides of ocean basins. The dynamics and physics of these boundary currents are different, and the ways of monitoring those currents are different. There are a variety of monitoring methods, including a repeated XBT/XCTD section, a moored current meter array, an integral measuring CTD mooring array in combination with inverted echo sounders with pressure gauges (PIES's), an underwater cable, a shipboard acoustic Doppler current profiler (ADCP), a regional acoustic tomography, RAFOS floats, and satellite altimetry. Examples selected here are the Kuroshio, East Australian Current, Indonesian Throughflow and North Brazil Undercurrent.*

1 - INTRODUCTION

Boundary currents are an important and integral part of the global oceanic three-dimensional circulation scheme. They advect substantial amounts of heat and mass between both hemispheres. Their fluctuations are prime agents for climatic changes. The observation of boundary currents at selected sites is essential for the definition of initial conditions needed for climate forecast models. There are a variety of boundary currents, including surface, intermediate and deep boundary currents on both western and eastern sides of ocean basins, and also interior boundary currents. Table 1

Table 1. Classification of boundary currents (BC) with some examples

	Western BC		Eastern BC	
Surface BC - intermedciate influence on climate	Gulf Stream	swift; O (100 km/d)	Canary C.	relatively slow; O (10 km/d)
	Kuroshio	deep (>2000 m)	California C.	less deep (<500 m)
	Agulhas C.	large transport (>50 Sv)	Benguela C.	low transports (<10-20 Sv)
	Brazil C.	sharp boundaries	.	different regime
	.	with coastal circulation	.	near boundaries
	.		.	
	.			parts of upwelling regions
Intermediate and Deep BC - indirect (long-term) impact on climate	No-name compensation currents as part of the global circulation			
	IWBC of the South Atlantic or South Indian	AAIW	Poleward Undercurrents	upwelling related
	DWBC of the Atlantic	NADW		
Interior BC - unknown impact on climate	Currents under control of mid oceanic ridges			

Abbreviations:
IWBC   Intermediate Western Boundary Current
DWBC   Deep Western Boundary Current
AAIW   Antarctic Intermediate Water
NADW   North Atlantic Deep Water

summarizes briefly the features of those boundary currents. The dynamics and physics of these boundary currents are different, and so the ways of monitoring those currents are different.

There are a variety of monitoring methods, including a repeated XBT/XCTD section, a moored current meter array, an integral measuring CTD mooring array in combination with inverted echo sounders with pressure gauges (PIES's), an underwater cable, a shipboard acoustic Doppler current profiler (ADCP), a regional acoustic tomography, RAFOS floats, and satellite altimetry. One of the cost-effective and practical ways of boundary current monitoring for heat and freshwater fluxes is a high resolution XBT/XCTD transect combined with a shipboard ADCP.

Examples selected here are the Kuroshio, East Australian Current, Indonesian Throughflow and North Brazil Undercurrent.

The Kuroshio is the (surface) western boundary current of the subtropical gyre of the North Pacific. Recently, the ASUKA Group carried out a set of measurements across the Kuroshio south of Japan. The transport of the Kuroshio is determined by geostrophic calculation using the repeated hydrographic survey data referenced to velocities observed by current meters moored at mid and abyssal depths. A procedure was developed to estimate a time series of volume transport of the Kuroshio from the TOPEX/POSEIDON altimetry data, based on a correlation between the measured transport and the difference in sea surface height across the Kuroshio. The Kuroshio transport will be monitored also with tide-gauge and submarine cables at several locations.

The East Australian Current is the (surface) western boundary current of the subtropical gyre of the South Pacific. Three high resolution XBT transects have been maintained for 7-13 years across the East Australian Current twice (Brisbane-Fiji and Sydney-Wellington) along the Australian coast and once (Auckland-Fiji) where the current has separated from the Australian coast and reattached at New Zealand. Present analysis is focusing on East Australian Current transport monitoring using a combination of the XBT data with TOPEX/POSEIDON altimetry and coastal tide gauge data.

The Indonesian Throughflow is closely related with western boundary currents of the Pacific and considered here as a boundary current. Due to the complexity of the bathymetry as well as the low latitude of the entrance channels, monitoring the Throughflow is challenging. The longest record of Throughflow mass and temperature transport is based on a repeated XBT transect between Australia and Java. Monitoring sea-level on each side of the major Throughflow straits by a shallow pressure gauge array could be the most cost-effective means of monitoring transport.

The North Brazil Undercurrent is the intermediate western boundary current in the tropical South Atlantic and considered to feed the warm water to the North Brazil Current, which carries water of South Atlantic origin across the equator. Under the program of the Climate Observing System for the Tropical Atlantic (COSTA) of CLIVAR, the oceanic current system such as the meridional overturning circulation in this western equatorial Atlantic will be surveyed in details. Eddy resolving RAFOS floats may be optimally suitable for monitoring those narrow boundary currents.

2 - KUROSHIO

The North Equatorial Current flowing westward broadly meets in the westernmost region of the North Pacific and forms a strong boundary current southeast of Taiwan. This western boundary current is called the Kuroshio. The primary part of this current in a shallow layer above 1000 m or less enters the East China Sea, proceeds northeastward along the continental slope, and flows out to the North Pacific through the Tokara Strait. The deep part of the boundary current flows along the eastern slope of the Ryukyu Ridge outside the East China Sea. This may partly or wholly join the Kuroshio flowing out from the East China Sea through the Tokara Strait, and may compose a deep part of the Kuroshio south of Japan.

Recently, a group called ASUKA (Affiliated Surveys of the Kuroshio off Cape Ashizuri) endeavored to measure the Kuroshio and its recirculation south of Shikoku, Japan, and estimate their absolute volume and heat transports (Imawaki et al., 1977; 1999). The observation line (Fig. 1) was chosen to coincide with a subsatellite track of the altimetry satellite TOPEX/ POSEIDON, which has been measuring the sea surface
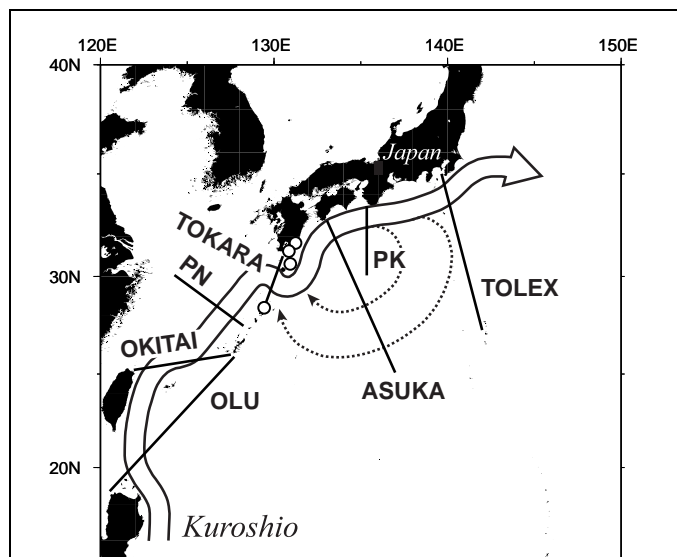

Fig. 1. Observation lines across the Kuroshio. TOLEX: ferry ADCP line; PK: hydrographic section; ASUKA: *in situ* and satellite monitoring line; TOKARA: ferry ADCP line; PN: hydrographic section; OKITAI and OLU: underwater cable measurement line. Circles are tide gauge stations at the Tokara Strait.

height since 1992 (Fu et al., 1994). During 1993-1995, they maintained nine moorings equipped with 33 current meters along the observation line to start the intensive survey. During this two-year period, the ASUKA Group carried out hydrographic surveys along the line repeatedly, using CTD and/or XBT, in order to estimate upper layer velocities, which cannot be measured adequately by those moored current meters; totally 42 repeat sections were obtained for the Kuroshio region.

Geostrophic velocities are calculated from repeated hydrographic survey data, with reference to velocities observed at mid and abyssal layers. The profile of the sea surface dynamic topography (SSDT) is estimated on the basis of absolute geostrophic velocities at the sea surface. The volume transport of the Kuroshio for the upper 1,000 m depth is estimated from the absolute geostrophic velocities obtained above. Here the Kuroshio is simply defined as the entire eastward flow.

The estimated transport of the Kuroshio is found to have a very tight relationship with the SSDT difference across the Kuroshio. The estimated Kuroshio transport varies from 27 to 85 Sv for 25 selected hydrographic surveys carried out during two years. Fig. 2 is a scatter plot of the Kuroshio transport for the upper 1,000 m and SSDT difference across the Kuroshio. Their correlation coefficient is high, and the rms (root-mean-square) difference from the regression line (with a slope of 81 Sv/m) is small. This result comes from the fact that the total transport is almost proportional to the sea-surface transport per unit depth, which is proportional to the SSDT difference across the stream; in other words, the increase (or decrease) of the total transport results from proportional increase (or decrease) of all the layers of the Kuroshio.
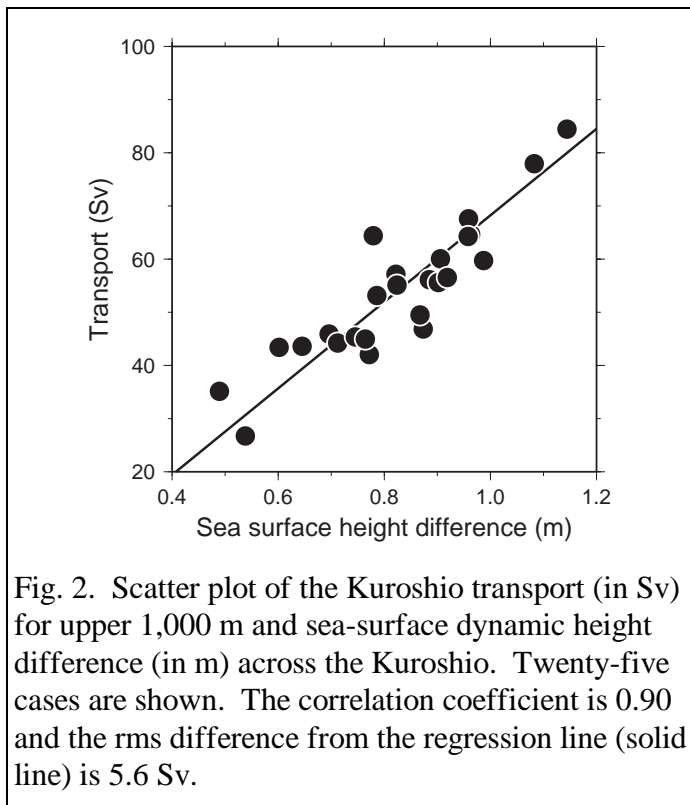

Fig. 2. Scatter plot of the Kuroshio transport (in Sv) for upper 1,000 m and sea-surface dynamic height difference (in m) across the Kuroshio. Twenty-five cases are shown. The correlation coefficient is 0.90 and the rms difference from the regression line (solid line) is 5.6 Sv.

Having this relationship, the SSDT difference across the Kuroshio derived from TOPEX/ POSEIDON altimetry data provides a time series of the Kuroshio transport with sufficiently fine resolution and as long a duration as the satellite operates. Fig. 3a shows a five-year record for 1992–1997 thus obtained, which is the first long-term record of the Kuroshio transport with sufficient temporal resolution. Altimeter-derived transports agree very well with transports estimated from in situ data. Sea level data at Cape Ashizuri are used to improve the SSDT profiles near the coast, where the altimeter cannot work well.

The Kuroshio transport fluctuates greatly around a mean of 57 Sv. Part of the transport is associated with the transport of the stationary local anticyclonic warm eddy located on the offshore side of the Kuroshio (Hasunuma and Yoshida, 1978). The present estimate of the Kuroshio transport necessarily includes the eastward transport of the northern part of this eddy, which is assumed to be equal to the westward transport of the southern part of this eddy, i.e., the westward-flowing Kuroshio recirculation. Activities of propagating cyclonic and anticyclonic mesoscale eddies are very high in this region. Most of the fluctuations shown above are associated with those mesoscale eddies, whose

contributions should also be excluded. The transport of the Kuroshio as the throughflow shows a smaller mean and smaller fluctuations. The transport of the westward-flowing Kuroshio recirculation is estimated in a similar way using the altimeter data and the relationship between the transport and SSDT difference obtained for the Kuroshio recirculation. The throughflow transport is estimated by subtracting this recirculation transport from the above-estimated Kuroshio transport (Fig. 3b). The five-year mean of the transport is estimated to be 42 Sv. The transport and its variability are reduced, in comparison with those of the Kuroshio as the eastward flow.

The present favorable relationship between the Kuroshio transport and SSDT difference across the Kuroshio provides a practical way of long-term monitoring of the transport using satellite altimeter
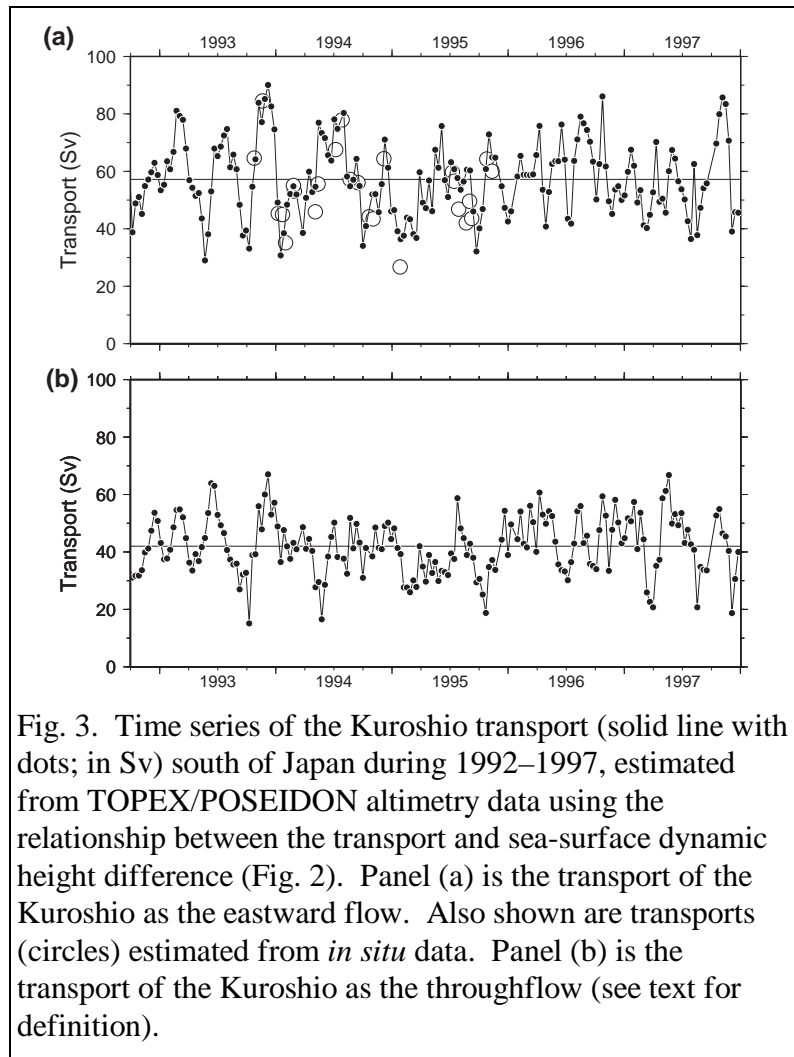

Fig. 3. Time series of the Kuroshio transport (solid line with dots; in Sv) south of Japan during 1992–1997, estimated from TOPEX/POSEIDON altimetry data using the relationship between the transport and sea-surface dynamic height difference (Fig. 2). Panel (a) is the transport of the Kuroshio as the eastward flow. Also shown are transports (circles) estimated from *in situ* data. Panel (b) is the transport of the Kuroshio as the throughflow (see text for definition).

data. A similar relationship has been previously suggested between the relative transport and SSDT difference for the Kuroshio (Nitani, 1975). A very similar combination of estimates of transport and SSDT difference for the Kuroshio south of Japan is found recently in a global ocean circulation model (P. Saunders, personal communication, 1998). A similar significantly linear relationship is also found for the Kuroshio east of Taiwan from recent field measurement WOCE PCM1 (Johns, et al., 1999). Such a relationship may hold more or less for most western boundary currents.

Sea level data from tide gauges (Fig. 1) south of Kyushu are useful to monitor the volume transport of the Kuroshio in the East China Sea. Regression equations for the Kuroshio transport were obtained by fitting to the geostrophic transport in the East China Sea observed and computed by the Nagasaki Marine Observatory, Japan Meteorological Agency. They were used for a study of the large meander of the Kuroshio by Kawabe (1995). The regressions show that the volume transport is estimated reasonably well with the sea level difference between the both sides of the Kuroshio.

Measurement of the voltage generated by electromagnetic induction due to ocean water movement, using a submarine cable, is effective to monitor the volume transport of the current flowing over the cable, and has been carried out in the Strait of Dover, the Straits of Florida, the Tasman Sea, and so on. Monitoring the Kuroshio transport using this method is just beginning. The voltage measurement started in June 1998 for submarine cables between Okinawa and Taiwan (OKITAI cable) and between Okinawa and Luzon (OLU cable) (Fig. 1). The following two subjects must be done before estimating transport. First, the noises from magnetic storms and earth currents like

spikes must be removed from the voltage data. The correction with geomagnetic data is being tried. Second, the voltage must be converted to volume transport. We will have the equations for the conversion by observing the volume transport over the cables with a free-falling sonde, lowered and shipboard acoustic Doppler current profilers, and CTD. The first observation will be made in September 2000 with R/V Hakuho Maru.

Hydrographic surveys of the Kuroshio have been carried out at several locations, including PK and PN lines (Fig. 1), since mid-1950's by Japan Meteorological Agency. Since 1970's, surveys have been carried out four times a year. Those will be continued in future. Upper layer velocities of the Kuroshio have been measured by ADCP's on ferry boats along TOLEX and TOKARA lines (Fig. 1) since early 1990's. Those surveys will also be continued in future.

3 - EAST AUSTRALIAN CURRENT

The western boundary current of the South Pacific subtropical gyre is sampled by a series of three high resolution XBT transects crossing the current at widely spaced locations (Fig. 4). The East Australia Current flows southward along the east coast of Australia, crossing line PX30 at Brisbane (26.6° S) and line PX34 at Sydney (33.9° S). The current separates from the coast before reaching Sydney, but it overshoots the XBT line southward before turning back to the northeast and recrossing PX34. Part of the separated current flowing eastward in the Tasman Front reattaches to the northern coast of New Zealand (Fig. 4) as the East Auckland Current, crossing the PX06 line at 35.5° S. Thus, the XBT transects capture the boundary current in three distinctly different domains. Fig. 4 shows the location of the three transects overlain on the temperature at 400 m, mapped from historical data. Quarterly sampling is carried out along each transect, beginning in 1986 along PX06 and in 1991 along PX30 and PX34. XBT profiles to 800 m are collected at intervals of 10 to 40 km along track.
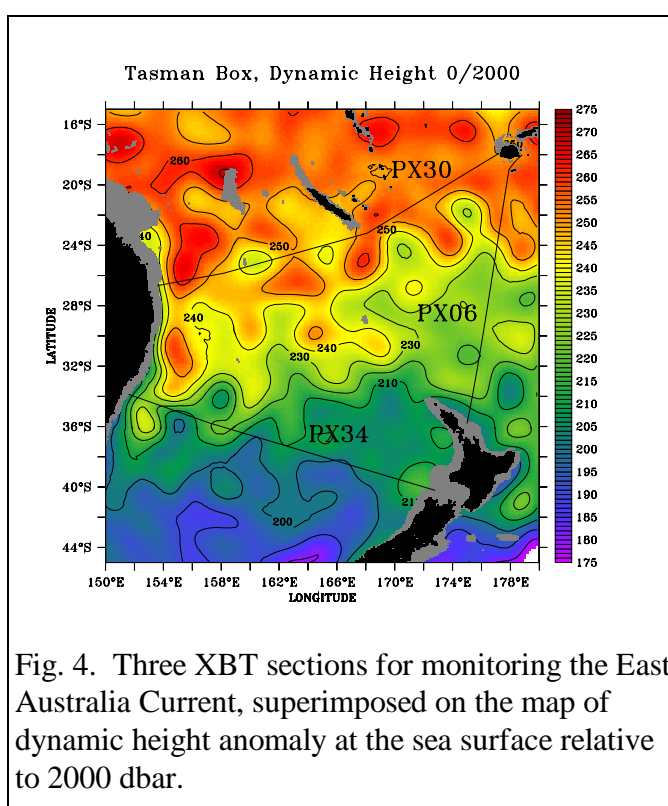

Fig. 4. Three XBT sections for monitoring the East Australia Current, superimposed on the map of dynamic height anomaly at the sea surface relative to 2000 dbar.

The mean and standard deviation of temperature fields for the three boundary current crossings are shown in Fig. 5. In each case, the mean current axis is located by the offshore drop in the height of isotherms, with a recirculation also seen on the offshore side of each crossing. The overall variability is highest at Sydney and lowest at Auckland. Interestingly, the variability is relatively low near shore in each transect, increasing to a maximum at the offshore side of each crossing.

The quarterly sampling of the high resolution XBT transects does not resolve variability in the boundary currents occurring on time-scales of days to months. While the focus of the sampling program is on seasonal-to-interannual variability, it is necessary to account for the aliased frequencies. Present analyses focus on using TOPEX/POSEIDON altimetric data to supplement the XBT transects in the time domain. Fig. 6 shows a comparison of XBT and TOPEX/POSEIDON

transport estimates for the East Auckland Current at the PX06 line. In the upper panel, a time-series of surface geostrophic velocity is shown, integrated from the inshore edge of the transect near the 200 m isobath, to the mean location of the offshore side of the current (35.6° S to 33.6° S). Geostrophic velocity from XBT data is relative to 800 m. Surface geostrophic velocity from TOPEX/POSEIDON is adjusted to have the same temporal mean as for the XBT data. Good agreement is seen between the two time-series, including the disappearance of the current in mid-1997 when it meandered offshore. One can also see that the altimeter captures substantial variability on time-scales shorter than three months, e.g. in late 1994 and early 1995. The lower panel of Fig. 6 shows similar time-series except the transport is over the depth range 0-800 m.
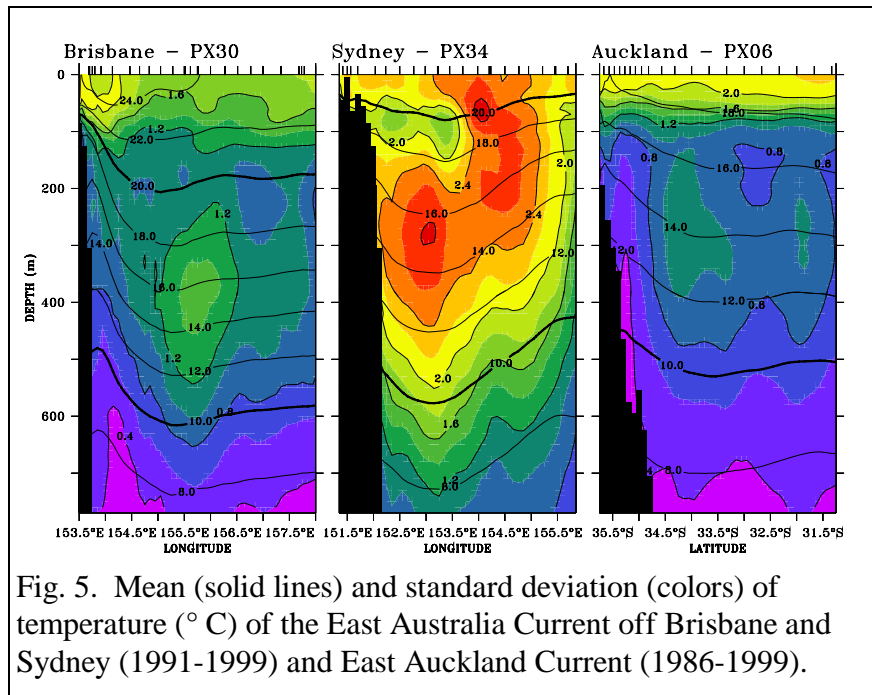

Fig. 5. Mean (solid lines) and standard deviation (colors) of temperature (° C) of the East Australia Current off Brisbane and Sydney (1991-1999) and East Auckland Current (1986-1999).

For this estimate, TOPEX/POSEIDON surface height is used together with a correlation function relating surface height anomalies to subsurface density structure to estimate the deep flow field. Again, it is seen that the TOPEX/POSEIDON and XBT series are in reasonable agreement.

A second limitation of the XBT transects is their 800 m depth range. It is clear from the mean temperature structure (Fig. 5) that the boundary currents extend deeper than 800 m. To date, top-to-bottom CTD measurements have been made along two of the lines. WOCE hydrographic project line P14C followed XBT line PX06 in September of 1992. Line PX30 was occupied with deep CTD stations by R/V Franklin (CSIRO) in January 1999. Plans are for a similar occupation of the PX34 line in 2001. Although these are one-time hydrographic transects, they provide
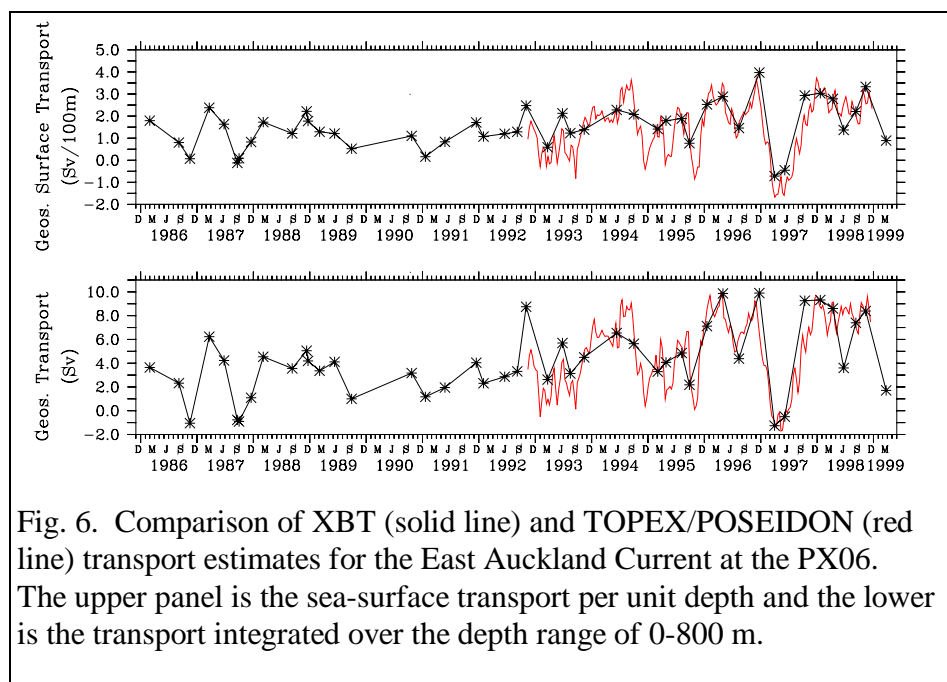

Fig. 6. Comparison of XBT (solid line) and TOPEX/POSEIDON (red line) transport estimates for the East Auckland Current at the PX06. The upper panel is the sea-surface transport per unit depth and the lower is the transport integrated over the depth range of 0-800 m.

valuable information on the deep structure of the boundary currents that is useful in interpreting the XBT and TOPEX/POSEIDON data sets. Plans for continued sampling along the XBT transects call for the use of new 2000 m probes and for salinity profiling in the surface layer. High resolution XBT transects provide a cost effective means of observing western boundary current structure and variability on seasonal to interannual time-scales. Similar sampling is being carried out along single tracks in the North Pacific and North Atlantic Ocean, with plans for comparable crossings in the South Indian and South Atlantic. An advantage of these transects is that they do not end at the offshore side of the current. They extend far offshore, in most cases to the other side of the ocean, in order to enable calculation of net transport of mass and heat for the combination of western boundary and interior ocean circulations.

4 - INDONESIAN THROUGHFLOW

The passages in the Indonesian Island chain allow the exchange of mass, heat and freshwater between the tropical Indian and Pacific oceans and so comprise the only major low-latitude inter-basin ocean pathway. This Indonesian Throughflow (hereafter ITF) impacts on the heat and freshwater budgets of these large ocean basins, both their long term means and on interannual timescales (Godfrey, 1996). Coupled modelling work by Schnieder (1998) reveals the large impact of the ITF on the global climate system (Fig. 7). By removing heat from the equatorial Pacific and warming the Indian oceans, deep atmospheric convection moves to the far western Pacific and Eastern Indian oceans. This shift in convection drives changes in the global atmospheric circulation and affects mid-latitude winds. Thus the ITF is a major player in controlling the heat content of the tropical Pacific and Indian oceans and so likely plays a role in the growth and dissipation of interannual anomalies such as El Nino.
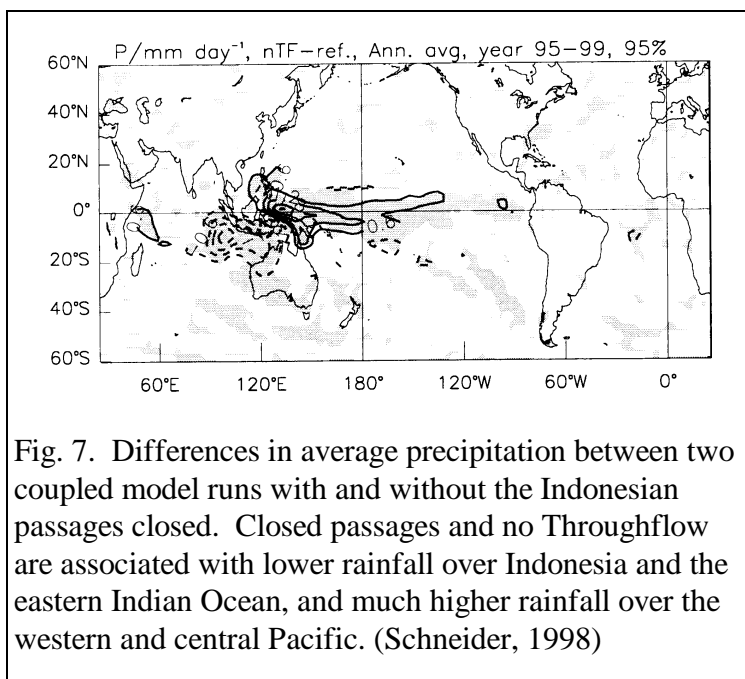

Fig. 7. Differences in average precipitation between two coupled model runs with and without the Indonesian passages closed. Closed passages and no Throughflow are associated with lower rainfall over Indonesia and the eastern Indian Ocean, and much higher rainfall over the western and central Pacific. (Schneider, 1998)

Efforts to constrain the heat and freshwater budgets of the Indian and Pacific oceans using ocean data are greatly hampered by lack of knowledge of the longterm mean ITF (Bryden and Imawaki, 1999; Wijffels, 1999), which is estimated to effect a heat transport of about 0.5 PW (Godfrey, 1996) from the Pacific to Indian oceans.

Monitoring the ITF and its associated heat and freshwater fluxes are thus needed:
To close the heat and freshwater budgets of the Pacific and Indian Ocean basins and thus better constrain integral surface fluxes,
To understand how anomalies of heat and freshwater content are exchanged between the Pacific and Indian oceans and what impact they have on air-sea interaction in these basins, and
To constrain climate models and so gain confidence in their ability to simulate the above.

Meyers et al. ["A Southern Hemisphere Perspective: monsoon, seasonal and interannual applications", this book] consider the broader issues of heat storage and air-sea exchange in the ITF region, while this paper concentrates on monitoring the inter-ocean exchange.

4.1 - Past and Present Attempts

Attempts to measure the ITF directly must grapple with the fact that the flow occurs in a topographically complex region where several possible pathways exist. The entrance channels on the Pacific side are near the equator making it impossible to rely on geostrophy as a means of estimation of the ITF and associated climate fluxes there. In the Indian Ocean, the outflow channels are at latitudes of 6°or higher, thus supporting the use of geostrophy. Meyers (1996) has monitored the upper portion of the ITF using an XBT line established in 1984 as part of the TOGA-TAO network. This line, designated as IX1 (Fig. 8a), is the basis for constructing the longest continuous estimate of the upper part of the ITF (Meyers and Pigot, 1999). With roughly fortnightly sampling this data set has been used to resolve changes in transport and heat content on bimontly timescales, adequate for resolving the seasonal and interannual changes in the ITF (Fig. 8b). Due to the depth limitation of XBT's only geostrophic transport between 0 - 400m has been estimated and density was derived using climatological salinities (Levitus, 1982). The latter is known to be problematic due to large smoothing scales. There is also a general lack of high quality salinity data at the northern end of IX1, increasing the uncertainty in estimating the T/S relationship.

Under the JADE and WOCE programs hydrographic lines were completed along or near IX1 and so provided synoptic estimates with full salinity (Fieux et al, 1996; Wijffels, et al., 1996). As was found by Fieux et al. (1996); use of climatological salinity data in the upper 800db results in transport errors of up to 5 Sv. The largest contributor to these
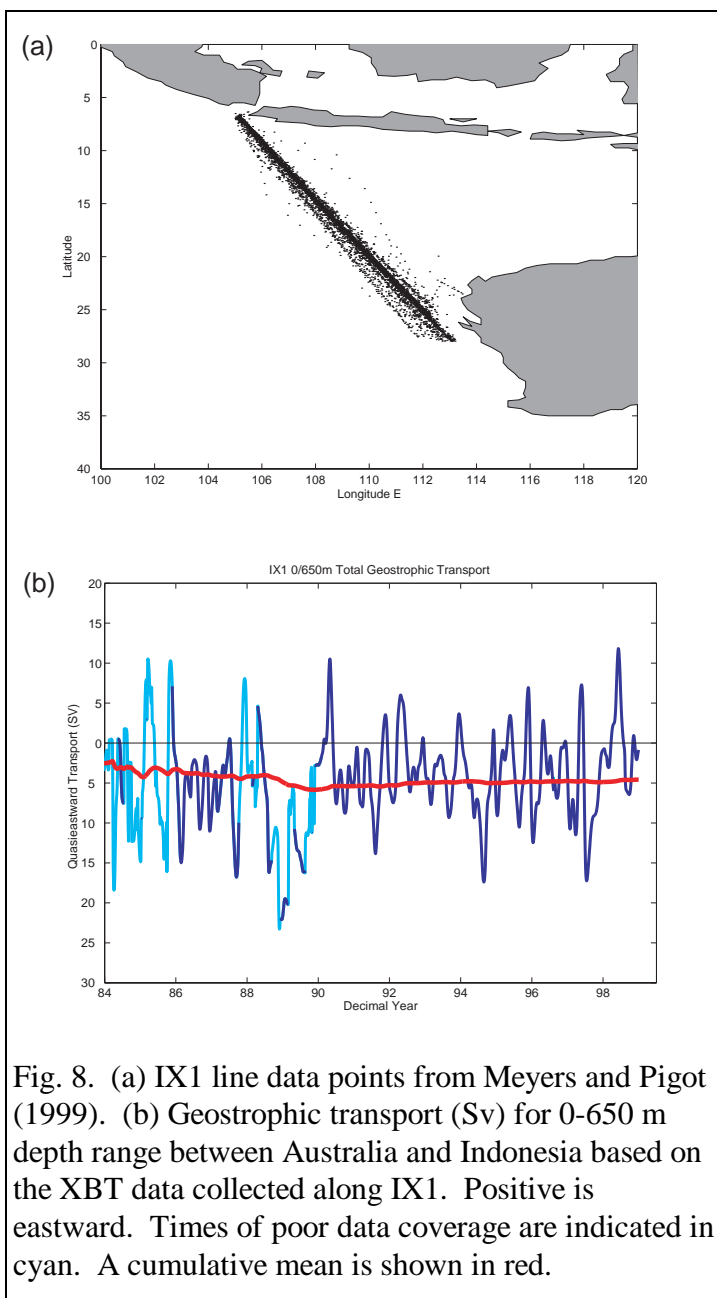

Fig. 8. (a) IX1 line data points from Meyers and Pigot (1999). (b) Geostrophic transport (Sv) for 0-650 m depth range between Australia and Indonesia based on the XBT data collected along IX1. Positive is eastward. Times of poor data coverage are indicated in cyan. A cumulative mean is shown in red.

errors is at the northern end of the section where a poorly understood boundary flow exists: the South Java Current. In the South Java Current, at the northern end point of IX1, conditions exist that are characteristic of the eastern equatorial Indian Ocean: an extremely thin thermocline separates a freshcap from salty North Indian subthermocline waters below. From a one year pilot mooring,

Sprintall et al. (1999) show large variations in salinity in the South Java Current, where at times, the freshcap disappears altogether under upwelling conditions. Hence, there appears to be considerable variability in the T/S relation at the northern end of IX1 which in turn must impact on the accuracy of the resulting transport estimates.

Despite this, Meyers (1996) has been able to link changes in thermal structure and transport along IX1 to large-scale wind-field variations over the tropical Pacific and Indian oceans. Meyers' results support predictions based on simple theory that remotely forced wind-driven Kelvin waves in both the Pacific and Indian oceans can drive changes in the ITF (Hirst and Godfrey, 1994; Clarke and Liu, 1994). The 1984-1995 record-average ITF estimated between 0-400 m is only ~5 Sv, much lower than the ~15 Sv estimate based on observed wind stresses and the modified Sverdrup theory of Godfrey (1989). Along with errors due to salinity, this highlights the possibility of IX1 not sampling a large deep contribution to the ITF.

Several short 1-2 year direct velocity estimates have been obtained in various Throughflow Straits (Molcard, et al, 1996; Cresswell et al, 1993; Aung, 1999; Murray and Arief, 1988; Gordon and Susanto, 1999; Gordon et al, 1999). These direct flow measurements, with their high temporal resolution, resolve the short term variability that the XBT data misses. In many of the straits, tidal variations are very large (e.g., Gordon and Susanto, 1999) and so likely dominate any single velocity measurement. In addition, the heave associated with large internal tides (Ffield and Gordon, 1992) can introduce errors into geostrophic estimates based on profile data taken in the internal seas.

Variability on intraseasonal timescales (40-60 days) has been shown to be ubiquitous in the Indonesian Seas (Molcard et al., 1996; Watanabe et al., 1992) and along the Sumatra/Java coasts (Arief and Murray 1996; Chong, et al., 1999). These oscillations impose a minimum temporal resolution of about 15 days (2-4 points per cycle) in order to avoid aliasing.

The vertical extent of the ITF, crucial to the associated heat flux, is still very poorly known. Cresswell et al. (1993) and Molcard et al. (1996) find 2-3 Sv flowing west in the Timor Passage below about 400 m. Fieux et al. (1996) find weak westward flow below 400 m in August 1989 but deduce eastward flow at these depths in February 1992.

An attempt has been made to use bottom pressure and inverted echo sounders (PIES) in Makassar Strait. This approach is still being assessed. The occurrence of seasonal shear reversals in the upper 250 m complicates the relationship between the integral measures obtained from the PIES and transport.

To date, it has not been possible to assess the accuracy of the transports measured by the IX1 line with direct measurements in the straits themselves. Except in the surface layers (Chong et al., 1999), the outflow channels (Lombok, Ombai and Timor) have never been simultaneously monitored, while the inflow channels are more numerous and much wider (Makassar, Maluku , Lifamatola and Halmahera). Based on water mass distributions, however, Gordon et al. (1999) suggest the bulk of the thermocline ITF flows through Makassar Strait. Strong coherence between two moorings placed on either side of the Libani Channel (a constriction in Makassar Strait) suggest a single mooring might be sufficient to monitor the Makassar Transport (Gordon and Susanto, 1999; Gordon et al., 1999). Due to storage effects between the IX1 line and the straits, it is not expected that transports will match, except at frequencies low enough for storage rates to be minimal, say 1-2 years.

Below we suggest monitoring activities aimed predominantly at measuring the oceanic fluxes. A more thorough discussion of these and other options is needed. The potential exists that inexpensive

proxy estimates of transport based on sea level, depth of thermocline or other indices, might be found, but these will require a relatively long and accurate direct estimate as a basis for calibration.

4.2 - Recommendations

4.2.1 - *Geostrophic estimates of the upper ITF*

We recommend continuing the IX1 XBT line at fortnightly sampling in order to reduce aliasing by the intraseasonal energy. Sampling should be supplemented with XCTDs especially north of 15°S. Inclusion of a thermosalinograph (TSG) might also help reduce errors due to large salinity variations in the surface layer. Model data could be used to determine the optimal mix of XCTD's, XBT's and TSG required to achieve accurate monthly estimates of mass, heat and freshwater fluxes.

 The idea of monitoring the ITF by measuring cross-strait pressure gradients is being explored through the shallow pressure gauge array established by Bray and colleagues (Chong et al., 1999). This array potentially represents an inexpensive means of monitoring near surface transports of mass, heat and freshwater through the straits, with high temporal resolution. Results are still preliminary, however, and more *in situ* verification of the deduced fluxes is required. The major problem with this technique is lack of information about flows at depth which can be oppositely directed to those at the surface (Chong et al., 1999). Multimonth mooring time series are recommended to help 'calibrate' the pressure gauge array under various seasonal and tidal regimes.

4.2.2 - *Direct estimates*

The geostrophic monitoring should be complemented by a direct estimate as an independent check and to fully resolve intraseasonal and higher frequency events. There are several locations where this could be achieved: long-term direct monitoring of the Makassar and Lifamatola Throughflow; and moorings in the three major outflow channels (Lombok, Ombai and Timor Straits). Gordon et al. (1999) show that monitoring the Makassar Throughflow could be feasible with a single mooring. Less is known about the structure of the Throughflow in Lifamatola Strait, which is quite wide at thermocline levels. However, water mass measurements suggest this strait is a significant pathway for the deep Throughflow.

Directly monitoring the deep Throughflow - that is the part not passing Through Makassar Strait - is a challenge and requires further study. It is likely new field work is required to determine the primary pathways of the deep Throughflow and to assess the feasibility of various monitoring approaches.

Profiling mooring technology (Fougere and Toole, 1998) could offer an alternative means of efficiently monitoring the full depth baroclinic component of the ITF. Profiling moored-CTDs are capable of delivering full depth profiles with daily or less frequently. Four such instruments moored on either side of the Savu Basin (Ombai outflow) and the Timor Trough, would provide the basis for bottom relative estimates of the ITF through these basins. Because full depth temperature and salinity profiles are obtained, heat and freshwater transports could also be derived. Such an array would have to be suitably programmed to avoid tidal aliasing. Along with a complementary means of monitoring the Lombok outflow through either a mooring or shallow pressure gauge array, full depth estimates of the Throughflow would be possible.

5 - NORTH BRAZIL CURRENT

It is well known that the low latitudes of the western South Atlantic play a decisive role in the oceanic inter-hemispheric exchange. They are part of the global meridional thermohaline circulation with its cold water limb in form of southward flowing North Atlantic Deep Water (NADW). Below the NADW level (> 3600 m) the coldwatersphere hosts Antarctic Bottom Water (AABW) which progresses northward compensating the import of NADW from the North Atlantic. This compensation is enhanced in the warmwatersphere by Antarctic Intermediate Water (AAIW) and thermocline waters which flow antiparallel to NADW in the upper kilometer (Schmitz, 1995). Fig. 9
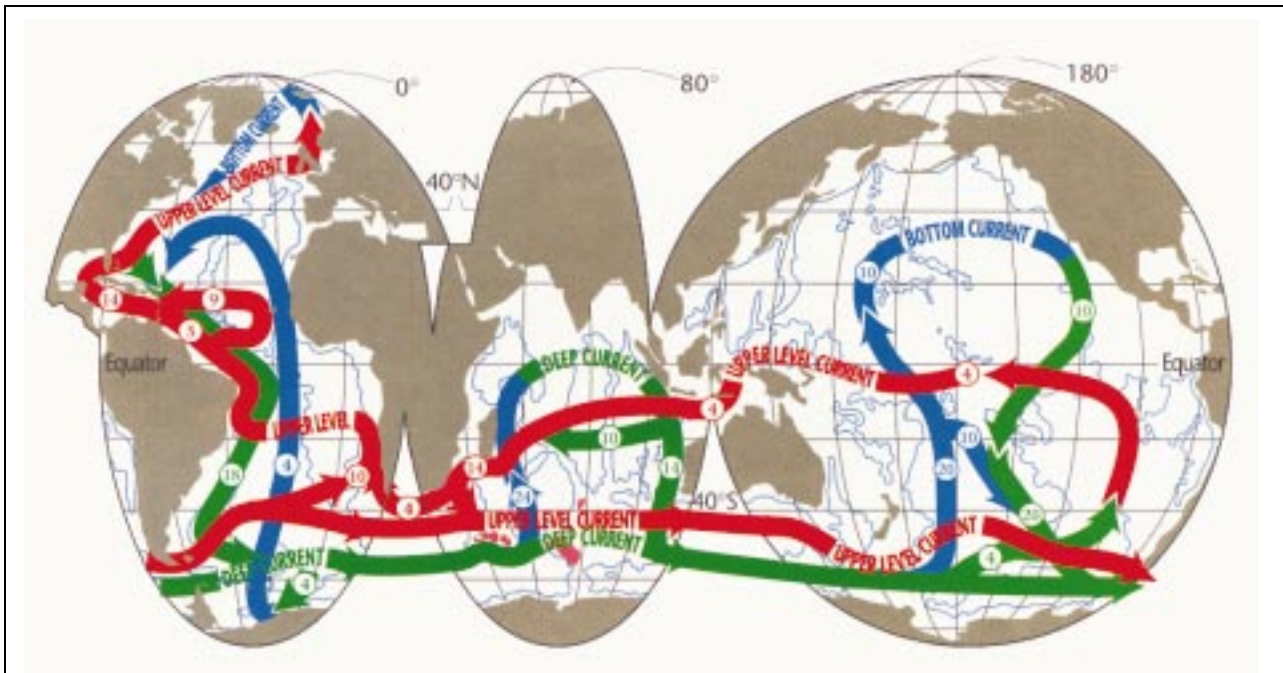

Fig. 9. Conceptual diagram of the three-dimensional oceanic circulation (Schmitz, 1995). Note the anti-parallel flows east of the continental slope off North Brazil. The boundary current system is represented by North Brazil Undercurrent at intermediate depth and the underlying flow of the North Atlantic Deep Water. The lower latitudes of the western South Atlantic are well predestinated for observations of the western boundary currents and their climate-relevant fluctuations.

shows a conceptual diagram of the three-dimensional circulation of the world ocean.

Recent studies during WOCE in the western tropical South Atlantic between 5° - 20° S have revealed flow characteristics of well defined boundary currents (Stramma et al., 1995; Schott et al., 1998; Weatherly et al., 1999; Zangenberg and Siedler, 1998). From the level of NADW upward they show minor spatial variations and seem to be isolated from interior flows by an extended zone of persistent eddy activities (Boebel et al., 1999a) without considerable augmentation from the subtropics. Fig. 10 shows major tropical currents in the Atlantic schematically. Fig. 11 shows space-time averaged mean velocities for the western South Atlantic, based on a total of 170 float years of velocity data. Fig. 12 shows the horizontal NADW transport pattern, schematically, according to the data from Meteor cruise 15.
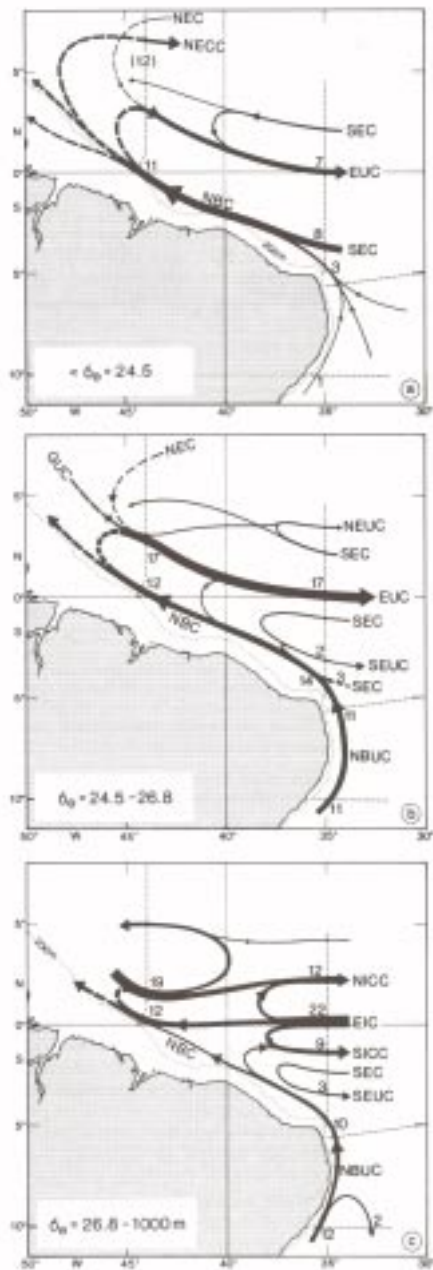
Fig. 10. Schematic map showing the major tropical currents for (a) the Tropical Surface Water layer at about 0 to 100 m for northern fall, (b) the Central Water layer at about 100 to 500 m depth, and (c) the Antarctic Intermediate Water and upper Circumpolar Deep Water range at about 500 to 1150 m depth. The figure demonstrates the limited eastern extent of the boundary current system without recognizable augmentation from the subtropical gyre. Shown are the North Equatorial Current (NEC), the North Equatorial Countercurrent (NECC), different branches of the South Equatorial Current (SEC), the Equatorial Undercurrent (EUC), the North Brazil Current (NBC), the Brazil Current (BC), the Guyana Undercurrent (GUC), the North Brazil Undercurrent (NBUC), the south Equatorial Countercurrent (SECC), the Equatorial Intermediate Current (EIC), the Northern Intermediate Countercurrent (NICC), and the Southern Intermediate Countercurrent (SICC) (from Schott et al., 1998).

These properties of the series of stacked boundary currents and clear topographical conditions off North Brazil predestinate the system as a choke point for monitoring its behavior. A group of oceanographers (F. Schott and collaborators) have chosen the region for observations of the tropical-subtropical coupling of the warmwatersphere. The project is a contribution to DecCen component of CLIVAR. It aims at the study of the reaction of the upper limb of the thermohaline circulation to natural perturbations. Impact model studies suggest a trigger process of climatic change as a consequence of fluctuating forcing functions.

During the most recently held WOCE workshop on the North Atlantic, a number of additional boundary current sites were suggested for moored current meter arrays. They include rigs off Labrador and off the Grand Banks. A report is being prepared by U. Send and M. Visbeck.
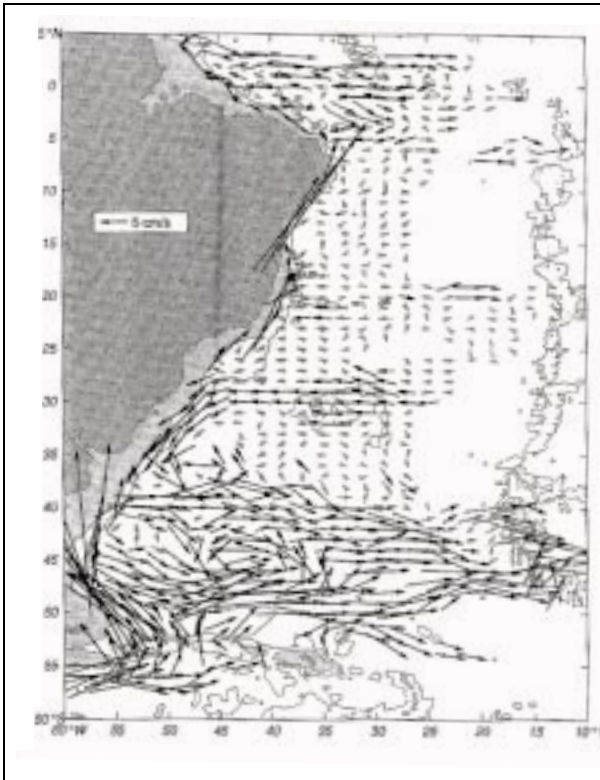
Fig. 11. Space-time averaged mean velocities based on a total of 170 float years of velocity data. For the interior ocean, away from the 1500 m isobath, the box size is 2° of latitude x 4° of longitude on a 1° x 1° grid. The arrows, based on at least 60 days of data, are centered at the respective box center and are red if the zonal component is eastward (blue if westward) and the speed is greater 3 cm/sec. along the western boundary at ~200 km intervals, data located between the coast and the 1500 m isobath was averaged within 200 km radius (black arrows, based on at least 15 days of data). Please note the confined lateral extension of the deep western boundary current in form of the North Brazil Undercurrent at 10° - 12° S (from Boebel et al., 1999b).
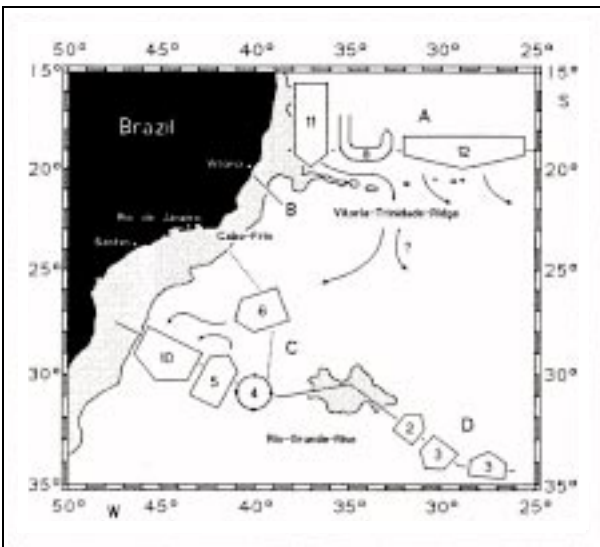

Fig. 12. Schematic horizontal NADW transport pattern according to the data from Meteor cruise 15. Values are rounded to full Sverdrup, and water depths less than 200 m are shaded. Note the broad drift of the NADW at 15° S. Its core seems to be separated from the slope (from Zangenberg and Siedler, 1998).

REFERENCES:

Arief, D. and S. P. Murray, Low-frequency fluctuations in the Indonesian throughflow through Lombok Strait. *J. Geophys. Res.*, 101, 12,455-12,464, 1996.

Boebel, O., R.E. Davis, M. Ollitrault, R.G. Peterson, P.L. Richardson, C. Schmid and W. Zenk, Direct observations of the intermediate depth circulation in the South Atlantic. *Geophys. Res. Letters* (accepted), 1999a.

Boebel, O., C. Schmid and W. Zenk, Kinematic elements of Antarctic Intermediate Water in the western South Atlantic. *Deep-Sea Res.* II, 46, 355-392, 1999b.

Bray, N. A., S. E. Wijffels, J. C. Chong, M. Fieux, S. Hautala, G. Meyers and W. M. L. Morawitz, Characteristics of the Indo-Pacific throughflow in the eastern Indian Ocean. *Geophys. Res. letters*, 24, 21, 2569-2572, 1997.

Bryden, H. L and S. Imawaki, Ocean transport of heat. Chapter 6.1 in "*Ocean Circulation and Climate*". Eds. J. A. Church and G. Siedler, Academic Press, London, (in Press), 2000.

Chong, J. C, J. Sprintall, S. Hautala, W. L. M. Morawitz, N. A. Bray and W. Pandoe, Shallow throughflow variability in the outflow straits of Indonesia, *Geophys. Res. Letters,* (submitted), 1999.

Clarke, A.J. and X. Liu, Interannual sea level in the northern and eastern Indian Ocean. *J. Phys. Oceanogr.*, 24, 1224-1235, 1994.

Cresswell, G., A. Frische, J. Petereson and D. Quadfasel, Circulation in the Timor Sea. *J. Geophys. Res.*, 98, 14,379-14,389, 1993.

Ffield, A. and A. L. Gordon, Tidal mixing signatures in the Indonesian seas. *J. Phys. Oceanogr.*, 26, 1924-1937, 1996.

Field, A. and A. L. Gordon, Vertical mixing in the Indonesian thermocline. *J. Phys. Oceanogr.*, 22, 184-195, 1992.

Fieux, M., R. Molcard and A. G.Ilahude, Geostrophic transport of the Pacific-Indian oceans throughflow. *J. Geophys. Res.*, 101, 12,421-12,432, 1996.

Fieux, M., C. Andrie, E. Charriaud, A. G. Ilahude, N. Metzl, R. Molcard and J. C. Swallow, Hydrological and chlorofluoromethane measurements of the Indonesian throughflow entering the Indian oceans. *J. Geophys. Res.*, 101, 12,433-12,454, 1996.

Fougere, A. J. and J. Toole, Physical oceanographic time-series sensors. *Sea Tech. Arlington VA*, 39, 2, 57-63, 1998.

Fu, L.-L., E.J. Christensen, C.A. Yamarone Jr., M. Lefebvre, Y. Menard, M. Dorrer, and P. Escudier, TOPEX/POSEIDON mission overview. *J. Geophys. Res.*, 99(C12), 24,369-24,381, 1994.

Godfrey, J.S., The effect of the Indonesian throughflow on ocean circulation and heat exchange with the atmosphere: A review. *J. Geophys. Res.*, 101, 12,217-12,237, 1996.

Godfrey, J.S., A Sverdrup model of the depth-integrated flow for the world ocean allowing for island circulations. *Geophys. Astrophys. Fluid Dyn.*, 45, 89-112, 1989.

Gordon, A. L. and R. D. Susanto, Makassare Strait Transport: Initial estimate based on Arlindo Results, *Marine Tech. Soc.*, 23, 34-45, 1999.

Gordon, A. L., R. D. Susanto and A. L. Ffield, Throughflow within Makassar Strait. *Geophys. Res. Letters*, (submitted), 1999.

Hasunuma, K. and K. Yoshida, Splitting of the subtropical gyre in the western North Pacific, *J. Oceanogr. Soc. Japan*, 34, 160-172, 1978.

Hirst, A. C. and J. S. Godfrey, The response to a sudden change in Indonesian throughflow in a global ocean GCM. *J. Phys. Oceanogr.*, 24, 1895-1910, 1994.

Imawaki, S., H. Uchida, H. Ichikawa, M. Fukasawa, S. Umatani and ASUKA Group, Time series of the Kuroshio transport derived from field observations and altimetry data, *Intl. WOCE Newsletter*, 25, 15-18, (Unpublished manuscript), 1997.

Imawaki, S., H. Uchida, H. Ichikawa, M. Fukasawa, S. Umatani, and ASUKA Group, Five-year record of the Kuroshio transport south of Japan, (in preparation).

Johns, W.E., T.N. Lee, D. Zhang, R. Zantopp, C.-T. Liu and Y. Yang, The Kuroshio east of Taiwan: Moored transport observations from the WOCE PCM-1 array, (submitted for publication), 1999.

Kawabe, M., Variations of current path, velocity, and volume transport of the Kuroshio in relation with the large meander. *J. Phys. Oceanogr.*, 25, 3103-3117, 1995.

Meyers, G., Variation of Indonesian throughflow and the El Nino-Southern Oscillation. *J. Geophys. Res.*, 101, 12,255-12,263, 1996.

Meyer, G. A. and L. Pigot, Analysis of Frequently Repeated XBT lines, http: / ~pigot/ REPORT, (unpublished manuscript), 1999.

Molcard, R., M. Fieux and A. G. Ilahude, The Indo-Pacific throughflow in the Timor Passage. *J. Geophys. Res.*, 101, 12,411-12,420, 1996.

Murray, S. P. and D. Arief, Throughflow into the Indian Ocean through the Lombok Strait, January 1985 - January 1986. *Nature*, 333, 444-447, 1988.

Nitani, H., Variation of the Kuroshio south of Japan, *J. Oceanogr. Soc. Japan*, 31, 154-173, 1975.

Quadfasel, D. and G. R. Cresswell, A note on the seasonal variability of the South Java Current. *J. Geophys. Res.*, 97, 3685-3688, 1992.

Schmitz, W.J., Jr., On the interbasin-scale thermohaline circulation. *Rev. Geophys.*, 33, 151-173, 1995.

Schott, F., J. Fischer and L. Stramma, Transports and pathways of the upper-layer circulation in the western tropical Atlantic. *J. Phys. Oceanogr.*, 28, 1904-1928, 1998.

Schneider, N., The Indonesian Throughflow and the Global Climate System, *J. Climate*, 11, 676-689, 1998.

Sprintall, J., J. Chong, F. Syamsudin, W. Morawitz, N. Bray and S. Wijffels, Dynamics of the South Java Current in the Indo-Australian Basin, *Geophys. Res. Letters*, (in press), 1999.

Stramma, L., J. Fischer and J. Reppin, The North Brazil Undercurrent. *Deep-Sea Res*. I, 42, 773-795, 1995.

Watanabe, H., Y. Kashino, H. Yamaguchi, M. Aoyama, B. Herunadi, K. Ando, K. Muneyama, and H. Mitsudera, Moored measurement of the Indonesian Throughflow at the southwestern edge of the Philippine Sea. *Intl. WOCE Newsletter*, 27, 26-30, (Unpublished manuscript), 1997.

Weatherly, G.L., Y.Y. Kim and E.A. Konter, Eulerian measurements of the North Atlantic Deep Water deep western boundary current at 18° S. *J. Phys. Oceanogr.* (in press), 1999.

Wijffels, S. E., N. Bray, S. Hautala, G. Meyers and W. M. L. Morawitz, The WOCE Indonesian Throughflow repeat hydrography sections: I10 and IR6. *Intl. WOCE Newsletter,* 24, 25-28. (Unpublished manuscript), 1996.

Wijffels, S. E., Ocean transport of fresh water. Chapter 6.2 in "*Ocean Circulation and Climate*". Eds. J. A. Church and G. Siedler, Academic Press, London, (in press), 2000.

Zangenberg, N. and G. Siedler, Path of the North Atlantic Deep Water in the Brazil Basin. *J. Geophys. Res*., 103 (C3), 5419-5428, 1998.